Spectroscopy, Photophysical Properties, and X-ray Crystal Structure of Platinum(II) Complexes of Quaterpyridine

Chin-Wing Chan and Chi-Ming Che*

Department of Chemistry, The University of Hong Kong, Pokfulam Road, Hong Kong

Ming-Chu Cheng and Yu Wang

Department of Chemistry, The National Taiwan University, Taipei, Taiwan

Received March 18, 1992

Two novel platinum quaterpyridine complexes have been synthesized and characterized by ^{1}H NMR spectroscopy and X-ray crystallography: $[Pt(pQP)](ClO_4)_2$ (*p*QP = 3″,5,5′,5‴-tetramethyl-2,2′:6′,2″:6″,2‴-quaterpyridine), monoclinic $C2/c$, a = 14.276 (2) Å, b = 12.970 (2) Å, c = 14.257 (1) Å, β = 102.29 (1)°, V = 2579.2 (6) Å^3, Z = 4; $[Pt(QP)](ClO_4)_2$ (QP = 2,2′:6′,2″:6″,2‴-quaterpyridine), monoclinic $P2_1$, a = 5.904 (3) Å, b = 12.943 (2) Å, c = 14.300 (4) Å, β = 100.70 (4)°, V = 1073.7 (6) Å^3, Z = 2. The shortest intermolecular Pt–Pt distances in $[Pt(pQP)](ClO_4)_2$ and $[Pt(QP)](ClO_4)_2$ are 7.249 (2) and 5.904 Å, respectively. Both complexes exhibit photoluminescence in the solid state at 700 nm. Only $[Pt(pQP)]^{2+}$ shows room-temperature emission in acetonitrile (ϕ_f = 0.026 ± 0.001, lifetime at infinite dilution = 7.0 ± 0.6 μs, self-quenching rate constant = 2.9 ± 0.4 × 10^8 M^{-1} s^{-1}). The excited state of $[Pt(pQP)]^{2+}$ is a powerful oxidant with an $E°$ value of about 2.3 V vs NHE.

Introduction

Polypyridine has actively been used as basic ligand for studies of electron-transfer and photochemical processes involving metal complexes.[1,2] Pyridine type ligands can serve as an "electron relay" due to their σ-donating and π-accepting properties.[3] Modification of substituents attached to the pyridine ring could lead to fine tuning of reactivities of the metal complexes. Recent efforts in the chemistry of metal–polypyridine complexes have also been directed to the synthesis of macrocycles containing bipyridine units in an attempt to encapsulate the metal center. The trend is to satisfy both electronic and steric demands of metal complex in various chemical and physical processes.[4]

Platinum(II) is known to be a catalytic and stoichiometric oxidation center to effect hydroxylation of unactivated C–H bonds.[5,6] However, better catalytic results can be obtained only when the detail mechanism is discovered.

In our way toward the design of new photooxidants, quaterpyridine and its derivatives have been picked up as ligand models. The covalent linkage of two bipyridyl units would improve electron delocalization and hence low-energy metal-to-ligand charge-transfer (MLCT) transitions would be anticipated. Here we describe two platinum(II) complexes of quaterpyridine which possess long-lived and emissive excited states.

Experimental Section

Materials. 2,2′:6′,2″:6″,2‴-Quaterpyridine (QP) and 3″,5,5′,5‴-tetramethyl-2,2′:6′,2″:6″,2‴-quaterpyridine (*p*QP)

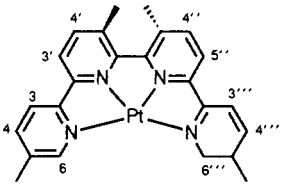

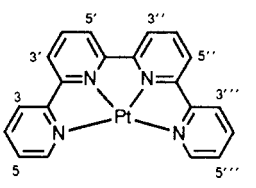

were synthesized according to literature methods.[7,8] K_2PtCl_4 and $LiClO_4$ were purchased from Aldrich. Acetonitrile for photophysical measurements was purified by distillation from $KMnO_4$ and CaH_2. Water for electrochemical studies was distilled from $KMnO_4$.

Physical Measurements and Instrumentation. Infrared spectra were measured in KBr pellets on a Nicolet 20 SXC FT-IR spectrometer. UV–visible spectra were obtained on a Milton Roy Spectronic 3000 spectrophotometer. Proton NMR spectra were obtained on a Jeol GSX 270 FT-NMR spectrometer with TMS as internal standard. Elemental analyses were performed by the Shanghai Institute of Organic Chemistry, Chinese Academy of Science.

Cyclic voltammograms were measured using a Princeton Applied Research (PAR) Model 175 universal programmer, Model 173 potentiostat, and Model 179 digital coulometer coupled to a Houston 2000 X-Y recorder. A conventional two-compartment cell was used in electrochemical measurements. A saturated calomel reference electrode (SCE) was used in aqueous media, while a silver–silver nitrate (0.1 M in acetonitrile) reference electrode was used in nonaqueous media with the ferrocenium–ferrocene couple as internal standard. The working electrode was either glassy carbon or pyrolytic graphite. The electrode surface was pretreated as described previously.[9]

Steady-state emission spectra were recorded on a Spex 1681 spectrofluorometer. Luminescence self-quenching was studied by measuring the emission lifetime as a function of the concentration of the platinum complex. The following equation was used to determine the self-quenching rate constant k_q:

$$1/\tau = 1/\tau_0 + k_q[Pt]$$

(1) Juris, A.; Balzani, V.; Barigelletti, F.; Campagna, S.; Belser, P.; von Zelewsky, A. *Coord. Chem. Rev.* **1988**, *84*, 85–277.
(2) Demas, J. N.; DeGraff, B. A. *Anal. Chem.* **1991**, *63*, 829A–837A.
(3) *Photoinduced Electron Transfer Part A*; Fox, M. R., Channon, M., Eds.; Elsevier: New York, 1988.
(4) Balzani, V.; Lehn, J. M.; van de Loosdrecht, J.; Mecati, A.; Sabbatini, N.; Ziessel, R. *Angew. Chem., Int. Ed. Engl.* **1991**, *30*, 190–191.
(5) Kao, L. C.; Sen, A. *J. Chem. Soc., Chem. Commun.* **1991**, 1242–1243.
(6) Labinger, J. A.; Herring, A. M.; Bercaw, J. *J. Am. Chem. Soc.* **1990**, *112*, 5628–5629.
(7) Lehn, J. M.; Sauvage, J. P.; Simon, J.; Ziessel, R.; Piccini-Leopardi, C.; Germain, G.; Declercq, J.-P.; Van Meersche, M. *Nouv. J. Chim.* **1983**, *7*, 413–420.
(8) Constable, E. C.; Elder, S. M.; Healy, J.; Tocher, D. A. *J. Chem. Soc., Dalton Trans.* **1990**, 1669–1674.
(9) Che, C. M.; Wong, K. Y.; Anson, F. C. *J. Electroanal. Chem.* **1987**, *226*, 211–226.

0020-1669/92/1331-4874$03.00/0

Table I. Crystal Data and Refinement Parameters

	$[Pt(QP)](ClO_4)_2$	$[Pt(pQP)](ClO_4)_2$
empirical formula	$PtN_4C_{20}Cl_2O_8H_{14}$	$PtN_4C_{24}Cl_2O_8H_{22}$
fw	704.35	760.46
space group	monoclinic $P2_1$	monoclinic $C2/c$
a (Å)	5.904 (3)	14.276 (2)
b (Å)	12.943 (2)	12.970 (2)
c (Å)	14.300 (4)	14.257 (1)
β (deg)	100.70 (4)	102.29 (1)
V (Å^3)	1073.7 (6)	2579.2 (6)
Z	2	4
d(calcd) (g/cm^3)	2.18	1.96
μ (mm^{-1})	6.91	5.76
λ (Å)	0.710 69	0.710 69
R_F[a]	0.024	0.041
R_w[b]	0.018	0.035
GoF[c]	1.61	3.1

[a] $R_F = \sum||F_o| - |F_c||/\sum|F_o|$. [b] $R_w = \{\sum w(F_o - F_c)^2/\sum wF_o^2\}^{1/2}$. [c] GoF = $\{\sum w(F_o - F_c)^2/(\text{no. of reflns} - \text{no. of params})\}^{1/2}$.

Table II. Atomic Parameters x, y, z and B_{iso} Values for the Non-Hydrogen Atoms of $[Pt(pQP)](ClO_4)_2$, Where Esd's Refer to the Last Digit Printed

	x	y	z	B_{iso}[a] (Å^2)
Pt	0	0.44919 (4)	0.25	4.79 (3)
N(1)	−0.0548 (5)	0.3657 (5)	0.1294 (5)	4.8 (4)
C(1)	−0.0561 (6)	0.2622 (7)	0.1202 (6)	5.2 (5)
C(2)	−0.0977 (7)	0.2044 (10)	0.0344 (8)	10.3 (9)
C(3)	−0.1342 (8)	0.2646 (10)	−0.0315 (10)	11.3 (9)
C(4)	−0.1411 (7)	0.3702 (10)	−0.0367 (7)	10.0 (9)
C(5)	−0.0970 (6)	0.4229 (7)	0.0469 (8)	7.3 (6)
C(11)	−0.1011 (9)	0.0968 (8)	0.0287 (9)	9.7 (4)
N(2)[b]	−0.0397 (8)	0.5620 (10)	0.1633 (9)	4.0 (3)
C(6)[b]	−0.0912 (10)	0.5392 (12)	0.0623 (11)	3.9 (3)
C(7)[b]	−0.1283 (13)	0.6158 (13)	0.0030 (14)	5.6 (5)
C(8)[b]	−0.1160 (12)	0.7144 (14)	0.0547 (14)	5.6 (5)
C(9)[b]	−0.0838 (18)	0.7608 (21)	0.1380 (21)	12.3 (9)
C(10)[b]	−0.0289 (10)	0.6586 (10)	0.1979 (10)	3.2 (3)
C(12)[b]	−0.0972 (15)	0.8475 (16)	0.1820 (16)	7.9 (6)
Cl	0.1919 (2)	0.1023 (2)	0.2005 (2)	6.4 (2)
O(1)	0.1081 (6)	0.0759 (7)	0.2190 (8)	14.1 (8)
O(2)	0.2646 (7)	0.0395 (10)	0.2416 (8)	19.0 (9)
O(3)	0.2132 (8)	0.2019 (8)	0.2316 (9)	18.9 (10)
O(4)	0.1888 (7)	0.0999 (8)	0.1046 (6)	15.8 (8)
N(11)[b,d]	−0.0651 (8)	0.5566 (10)	0.1159 (9)	4.0 (3)
C(12)[c]	−0.0958 (18)	0.4976 (21)	0.0553 (21)	2.5 (6)
C(13)[c]	−0.1442 (22)	0.5880 (22)	−0.0363 (23)	3.7 (7)
C(14)[c]	−0.1458 (20)	0.6937 (22)	0.0029 (22)	3.1 (6)
C(15)[b]	−0.0960 (11)	0.7318 (12)	0.1003 (12)	3.7 (4)
C(16)[c]	−0.0611 (22)	0.6598 (24)	0.1522 (24)	4.1 (7)
C(17)[b]	0	0.6678 (16)	0.25	3.5 (5)
C(18)[c]	−0.0541 (17)	0.7463 (19)	0.1804 (19)	1.9 (5)
C(19)[c]	−0.1079 (19)	0.6500 (21)	0.0352 (20)	2.5 (6)
N(20)[c]	−0.0228 (16)	0.5735 (16)	0.1896 (16)	3.4 (5)
C(21)[c]	−0.0646 (19)	0.8528 (21)	0.2423 (21)	2.9 (6)
C(21′)[c]	−0.1353 (23)	0.8383 (25)	0.123 (3)	4.6 (8)

[a] $B_{iso} = (^8/_3\pi^2)\sum_i\sum_j u_{ij}a_i^*a_j^*\mathbf{a}_i\cdot\mathbf{a}_j$. [b] Atoms with occupancy = 0.5. [c] Atoms with occupancy = 0.25. [d] Atom type is 50% C and 50% N.

Emission lifetime measurements were made using a conventional laser system. The excitation source was the 355-nm output of a Quanta-Ray DCR-3 pulsed Nd-YAG laser (10 Hz, G-resonator). The signals were recorded on a Tektronix Model 2430 digital oscilloscope and analyzed using a least-squares fit program. The quantum yield of emission was measured by the method of Crosby[10] with quinine sulfate in 0.1 N sulfuric acid as standard. Solutions for photophysical measurements were degassed with no fewer than three freeze–pump–thaw cycles.

Synthesis. $[Pt(pQP)](ClO_4)_2$ {[1]$(ClO_4)_2$}. A mixture of pQP (99 mg, 2.7×10^{-4} mol) and K_2PtCl_4 (146 mg, 3.5×10^{-4} mol) in an acetonitrile/water (1:1, 60 mL) mixture was refluxed for 24 h. The solution was then cooled, filtered, and treated with lithium perchlorate. Microcrystals were separated from solution when the later was concentrated in vacuo, which were filtered out and washed with a few milliliters of chloroform to remove any unreacted ligand. The yield was 115 mg (56%). Anal. Calcd for $C_{24}H_{22}N_4PtCl_2O_8$: C, 37.91; H, 2.92; N, 7.37. Found: C, 37.29; H, 2.63; N, 7.22. ^{1}H NMR (CH_3CN): δ 8.65 s, $^3J_{Pt-H}$ 27 Hz, (H6,6‴); δ 8.30–8.20 m (H3,4,3′,4′,4″,5″,3‴,4‴); δ 2.63 s, (5,5‴-Me and 5′,3″-Me). IR (cm^{-1}): 1488 m, 1143 s, 1089 s, 636 m, 625 m. UV–vis in CH_3CN [λ_{max}/nm (10^{-3} ϵ)]: 418 (1.3), 394 (2.4), 360 (15), 340 (17), 333 (23).

$[Pt(pQP)](CF_3SO_3)_2$. A mixture of pQP (12.5 mg, 3.4×10^{-5} mol) and K_2PtCl_4 (23.5 mg, 1.7 equiv) in an acetonitrile and water mixture (1:1, 20 mL) was refluxed for 10 h. The resulting solution was filtered while warm and was treated with $AgCF_3SO_3$ (60 mg, 2.34×10^{-4} mol). The mixture was warmed at about 70 °C for 30 min. The solution was concentrated to about 10 mL after removal of silver chloride by filtration. Diethyl ether (20 mL) was added to induced precipitation. Greenish yellow microcrystals (10.8 mg, 37% yield) were isolated after 2 days at 4 °C. ^{1}H NMR (D_2O): δ 8.59 s, (H6,6‴); δ 8.38–8.23 m, (H3,4,3′,4′,4″,5″,3‴,4‴); δ 2.63 s and 2.58 s (5,5‴-Me and 5′,3″-Me). IR (cm^{-1}): 1158 s, 1031 s, 636 s. UV–vis in CH_3CN [λ_{max}/nm (10^{-3} ϵ)]: 419 (0.61), 388 (1.8), 360 (12), 344 (8.5), 327 (8.6).

$[Pt(QP)](ClO_4)_2$ {[2]$(ClO_4)_2$}. A mixture of QP (80 mg, 2.58×10^{-4} mol) and K_2PtCl_4 (139 mg, 1.3 equiv) in an acetonitrile/water (1:1, 45 mL) mixture was refluxed for 6 h. Any particulate material was removed by filtration. Solution was concentrated to about 25 mL under reduced pressure and treated with excess lithium perchlorate to induced precipitation. The greenish yellow solid was filtered out, washed with water (3×5 mL), and air dried. Recrystallization from hot acetonitrile afforded microcrystals (50 mg, 28% yield). Anal. Calcd for $C_{20}H_{14}N_4PtCl_2O_8$: C, 34.11; H, 2.00; N, 7.95. Found: C, 34.28; H, 1.91; N, 8.07. ^{1}H NMR (CH_3CN): δ 8.88 dd (H6,6‴); δ 8.53–8.47 t (H4′,4″); δ 8.51–8.45 dt, (H4,4‴); δ 8.40–8.34 m (H3′,5′,3″,5″). IR (cm^{-1}): 1089 s, 787 m, 623 m. UV–vis in CH_3CN [λ_{max} (10^{-3} ϵ)]: 409 (0.61), 388 (1.8), 360 (12), 344 (8.5), 327 (8.6).

$[Pt(QP)](CF_3SO_3)_2$. A mixture of QP (80.8 mg, 2.6×10^{-4} mol) and K_2PtCl_4 (135.5 mg, 3.3×10^{-4} mol) was refluxed in an acetonitrile and water mixture (1:1, 45 mL) for 18 h. The solution was filtered and treated with $AgCF_3SO_3$ (350 mg, 13.2×10^{-4} mol) at 70 °C. After 30

Table III. Atomic Parameters x, y, z and B_{iso} Values for Non-Hydrogen Atoms of $[Pt(QP)](ClO_4)_2$, Where Esd's Refer to the Last Digit Printed

	x	y	z	B_{iso}
Pt	0.19500 (6)	0.31262	0.25933 (2)	2.91 (4)
N(1)	0.0575 (13)	0.4469 (5)	0.3057 (5)	3.2 (4)
N(2)	0.3647 (12)	0.4078 (5)	0.1998 (4)	2.7 (3)
N(3)	0.3738 (12)	0.2110 (6)	0.1987 (5)	3.6 (4)
N(4)	0.0746 (12)	0.1761 (5)	0.3023 (4)	2.9 (3)
C(1)	−0.0887 (16)	0.4634 (6)	0.3589 (5)	3.0 (4)
C(2)	−0.1601 (17)	0.5587 (7)	0.3836 (6)	4.0 (5)
C(3)	−0.0526 (20)	0.6493 (8)	0.3515 (7)	5.3 (6)
C(4)	0.1190 (18)	0.6381 (7)	0.2952 (7)	4.4 (5)
C(5)	0.1725 (18)	0.5411 (7)	0.2696 (7)	4.1 (5)
C(6)	0.3422 (14)	0.5131 (7)	0.2102 (5)	2.9 (4)
C(7)	0.4680 (17)	0.5828 (7)	0.1659 (6)	4.2 (5)
C(8)	0.6180 (17)	0.5419 (9)	0.1147 (7)	5.2 (6)
C(9)	0.6590 (16)	0.4338 (7)	0.1027 (6)	4.0 (5)
C(10)	0.5272 (15)	0.3717 (7)	0.1443 (6)	4.0 (5)
C(11)	0.5154 (15)	0.2568 (6)	0.1514 (6)	3.0 (4)
C(12)	0.6446 (17)	0.1862 (8)	0.1047 (7)	4.7 (6)
C(13)	0.6213 (17)	0.0857 (7)	0.1137 (6)	4.3 (5)
C(14)	0.4623 (18)	0.0459 (8)	0.1669 (7)	4.6 (5)
C(15)	0.3274 (18)	0.1124 (7)	0.2107 (7)	4.6 (5)
C(16)	0.1606 (15)	0.0973 (6)	0.2721 (6)	2.7 (4)
C(17)	0.0961 (18)	−0.0015 (7)	0.2962 (6)	4.2 (5)
C(18)	−0.0586 (17)	−0.0137 (7)	0.3523 (7)	4.6 (6)
C(19)	−0.1482 (19)	0.0672 (7)	0.3854 (6)	4.5 (5)
C(20)	−0.0916 (16)	0.1667 (8)	0.3609 (6)	4.1 (5)
Cl(1)	0.0556 (4)	0.3131 (10)	0.9280 (1)	4.3 (3)
O(11)	0.0647 (15)	0.2157 (6)	0.9751 (5)	7.0 (5)
O(12)	−0.1660 (12)	0.3122 (21)	0.8728 (5)	8.0 (8)
O(13)	0.0925 (13)	0.3968 (6)	0.9955 (5)	6.9 (4)
O(14)	0.222 (1)	0.312 (3)	0.8687 (6)	9.2 (7)
Cl(2)	0.5185 (5)	0.8083 (11)	0.4739 (2)	5.1 (2)
O(21)	0.4841 (13)	0.807 (3)	0.3736 (4)	7.3 (8)
O(22)	0.7471 (15)	0.834 (2)	0.5049 (5)	13.4 (8)
O(23)	0.5119 (18)	0.7064 (6)	0.5066 (7)	8.3 (5)
O(24)	0.3604 (23)	0.8620 (10)	0.5063 (9)	21.2 (13)

(10) Demas, J. N.; Crosby, G. A. *J. Phys. Chem.* **1971**, *75*, 991–1024.

Table IV. Selected Bond Lengths and Bond Angles for $[Pt(pQP)](ClO_4)_2$

Bond Lengths (Å)			
Pt–N(1)	2.041 (7)	N(2)–C(6)	1.50 (2)
Pt–N(1A)	2.041 (7)	N(2)–C(10)	1.34 (2)
Pt–N(2)	1.92 (1)	N(1)–C(5)	1.41 (1)
Pt–N(2A)	1.92 (1)	N(1)–C(1)	1.35 (1)
Bond Angles (deg)			
N(2)–Pt–N(2A)	80.8 (5)	N(1A)–Pt–N(2A)	81.6 (4)
N(1)–Pt–N(2)	81.6 (4)	Pt–N(2)–C(6)	119 (1)
N(1)–Pt–N(2A)	162.4 (4)	Pt–N(2)–C(10)	119 (1)
N(1)–Pt–N(1A)	116.0 (3)	Pt–N(1)–C(5)	116.2 (6)
N(1A)–Pt–N(2)	162.4 (4)		

Table V. Selected Bond Lengths and Bond Angles for $[Pt(QP)](ClO_4)_2$

Bond Lengths (Å)			
Pt–N(1)	2.078 (7)	N(2)–C(6)	1.38 (1)
Pt–N(2)	1.888 (6)	N(3)–C(11)	1.31 (1)
Pt–N(3)	1.984 (7)	N(3)–C(15)	1.324 (1)
Pt–N(4)	2.041 (6)	N(4)–C(16)	1.25 (1)
N(1)–C(1)	1.27 (1)	N(4)–C(20)	1.41 (1)
N(1)–C(5)	1.53 (1)	C(5)–C(6)	1.47 (1)
N(2)–C(10)	1.43 (1)	C(10)–C(11)	1.49 (1)
Bond Angles (deg)			
N(1)–Pt–N(2)	82.5 (3)	C(11)–N(3)–C(15)	132.1 (8)
N(1)–Pt–N(3)	164.8 (3)	C(16)–N(4)–C(20)	120.4 (7)
N(1)–Pt–N(4)	116.7 (3)	N(1)–C(5)–C(6)	112.9 (7)
N(2)–Pt–N(3)	82.3 (3)	N(2)–C(6)–C(5)	113.3 (7)
N(2)–Pt–N(4)	160.8 (3)	C(5)–C(6)–C(7)	125.4 (8)
N(3)–Pt–N(4)	78.5 (3)	C(9)–C(10)–C(11)	132.0 (8)
C(1)–N(1)–C(5)	117.4 (7)	C(10)–C(11)–C(12)	124.6 (8)
C(6)–N(2)–C(10)	118.1 (7)		

min, the solution was filtered and evaporated to about 25 mL under reduced pressure. Upon cooling of the mixture to 4 °C for 3 h, a yellow precipitate separated from solution, which was filtered out and washed with 1 mL of cool water. The yield was 83.5 mg (43%). ^1H NMR (D_2O): δ 8.59 s, (H6,6‴); δ 8.37–7.83 m (H3,4,3′,4′,5′,3″,4″,5″,3‴,4‴,5‴). IR (cm^{-1}): 1262 s, 1226 m, 1164 m, 1032 m, 792 m, 778 m, 636 m. UV–vis in CH_3CN [λ_{max} (10^{-3} ϵ)]: 410 (0.59), 390 (1.4), 360 (9.8), 344 (6.6), 326 (8.5).

X-ray Structure Determination. Crystals of $[1](ClO_4)_2$ were obtained by diffusion of diethyl ether into an acetonitrile solution. A yellow crystal of dimensions 0.30 × 0.30 × 0.20 mm was mounted on a glass fiber on a Enraf-Nonius CAD-4 diffractometer. Intensity data were collected using the $\theta/2\theta$ scan mode. Cell dimensions and the space group were determined from 24 reflections with $18.90 \leq 2\theta \leq 24.50$ (Table I). A total of 2376 reflections were collected, of which 2274 were unique and 1713 of these had $I_{net} > 2\sigma(I_{net})$. The data were corrected for absorption, and the structure was solved by Patterson and Fourier methods. The last least-squares cycle was calculated with 38 atoms and 184 parameters. Weights based on counting statistics were used.[11] The atomic coordinates and isotropic temperature parameters were listed in Table II.

Yellow needles of $[2](ClO_4)_2$ were grown from acetonitrile. A yellow crystal of dimensions 0.20 × 0.20 × 0.40 mm was mounted on a glass fiber on a Enraf-Nonius CAD-4 diffractometer. The intensity data were collected with the same instrument (see previous paragraph and Table I). Cell dimensions and the space group were obtained from 24 reflections with $18.70 \leq 2\theta \leq 23.39$. Intensity data were treated in the same way as before. A total of 2157 reflections were collected, of which 1956 were unique and 1675 of these had $I_{net} > 2\sigma(I_{net})$. The last least-squares cycle was calculated with 49 atoms and 316 parameters. Weights based on counting statistics were used. The atomic coordinates and isotropic temperature factors were listed in Table III. Selected bond lengths and bond angles of $[1](ClO_4)_2$ and $[2](ClO_4)_2$ were listed in Table IV and Table V, respectively.

(11) $[Pt(pQP)](ClO_4)_2$ is seriously disordered with 50% of the molecules in the crystal having C_2 symmetry, which is shown in Figure 1. All the selected bond lengths and angles (Table IV) are from this part of molecule. The other 50% of the molecules are very irregular in shape; in order to satisfy the crystallographic 2-fold symmetry, 25% of the molecules are unique (occupancy of 0.25 in Table II), the remaining 25% of the molecules are generated from the 2-fold axis.

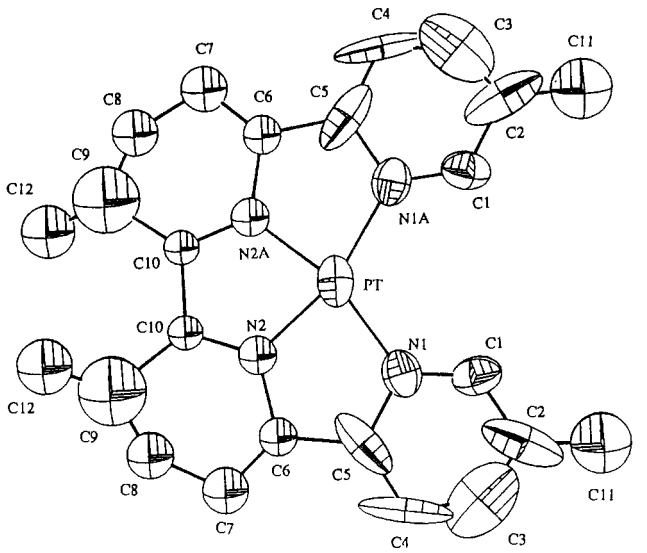

Figure 1. Perspective drawing of the $[Pt(pQP)]^{2+}$ cation with atom numbering.

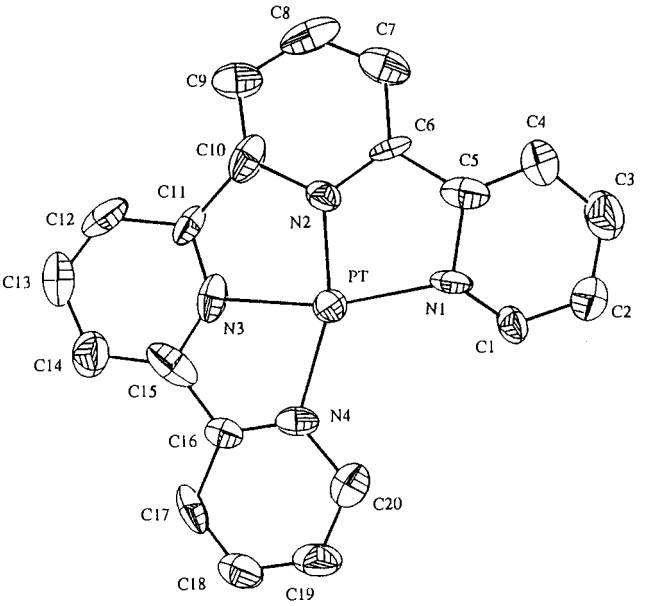

Figure 2. Perspective drawing of the $[Pt(QP)]^{2+}$ cation with atom numbering.

Results and Discussion

The syntheses and X-ray crystal structures of some metal–quaterpyridine complexes have been reported in several instances.[8,12] Figures 1 and 2 depict the ORTEP plots of **1** and **2**, respectively. Their crystal lattices and molecular dimensions are shown in Figures S1 and S2 (supplementary material). Stacking along the metal–metal axis in the solid form of (α-diimine)-platinum(II) complexes was well-known,[13] in which the short intermolecular Pt–Pt separation contributes to the intensive color and luminescence properties. However, the columnar structures observed in this study, though they exiset, are lengthened to a considerable extent determined by the molecular structure of the motifs.

Both PtN4 planes of **1** and **2** are essentially planar. Only a slight twisting of the ligand frame is observed in the latter. The dihedral angles between two halves of the ligand across the pseudo-

(12) (a) Maslen, E. N.; Raston, C. L.; White, A. H. *J. Chem. Soc., Dalton Trans.* **1975**, 323–326. (b) Lip, H. C.; Plowman, R. A. *Aust. J. Chem.* **1975**, *28*, 893.

(13) Che, C. M.; He, L. Y.; Poon, C. K.; Mak, T. C. W. *Inorg. Chem.* **1989**, *28*, 3081–3083.

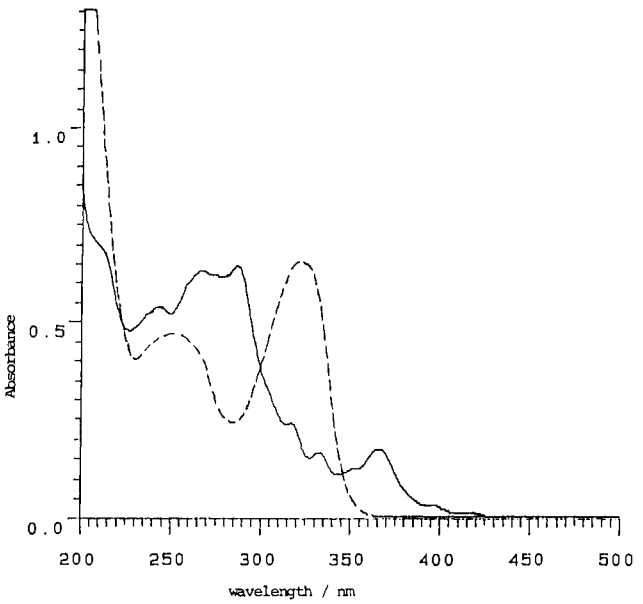

Figure 3. UV–vis absorption spectrum of $[Pt(pQP)]^{2+}$ (—, 10^{-4} M) and $[H_2(pQP)]^{2+}$ (- - -, 7×10^{-5} M) in acetonitrile at room temperature.

2-fold axis are 1.3 (2) and 5.8 (1)° for **2** and **1**, respectively. The irregular shape of **1** is most probably due to nonbonding interactions between the 5′- and 3″-methyls. They are displaced 0.93 (2) Å above and 0.91 (1) Å below the main plane defined by the PtN4 atoms. The steric bulkiness of these methyl groups opens up the interplanar separation of Pt stacks (see Figure S1). The result is extensive interculation among the columnar units within the lattice. This may lead to fractional occupancy and the disorder observed.[11]

The shortest Pt–Pt distances calculated in $[1](ClO_4)_2$ are 7.249 (2) Å, measured between adjacent columns, and 9.643 (2) Å, measured within the same columnar unit. The void so generated is filled by perchlorate anion, making the Pt–O distances 3.536 (7) and 5.129 Å (see Figure S1). In $[2](ClO_4)_2$, the Pt–Pt distance is 5.904 Å (see Figure S2), which is too long for any Pt–Pt interaction. However, this distance is shorter than the interplanar separation observed in the free quaterpyridine (6.35 Å),[7] suggesting the possibility of having ligand π–π interactions in the solid state.

It seems that significant Pt–Pt interaction in the solid state of Pt(II) polypyridine complexes occurs only when either the metal atom is bonded to three or less pyridyl units with the remaining coordination sites occupied by small molecules[13] or when the four coordinating aryl rings bow to one side for strain release.[14]

In-plane distortions have been observed in both complexed quaterpyridine units. The large deviation of bond angles from the free ligand indicates that the two terminal pyridyl rings are drawn toward the center. In **1**, the large reduction of twist compared with the corresponding dihedral angle (26°) found in $[Cu(pQP)(H_2O)](ClO_4)_2$[15] may be attributed to bending of the two internal pyridyl rings and a strong Pt–pyridyl interaction.

The NMR spectra of the platinum complexes indicate deshielding of aromatic protons on QP and *p*QP upon coordination of platinum (for assignments, see Experimental Section). Through-bond coupling (Pt–H) is observed in **1** only. The absence of the corresponding hyperfine interaction in $[Pt(QP)]^{2+}$ may be attributed to its planarity (the dihedral angle of H–C–C–Pt is almost zero).

Figure 3 shows the electronic absorption spectra of **1** and the diprotonated form of *p*QP (H_2pQP^{2+}) measured in acetonitrile at room temperature. The spectrum of **1** is very similar to that of **2** and bears resemblance to that of $[Pt(phen)_2](ClO_4)_2$ (phen = 1,10-phenanthroline).[16] For either **1** or **2**, there are several strong absorption bands from 200 to 300 nm which can be assigned to intraligand π–π^* transitions. Interestingly, there are low-energy absorption bands ranging from 340 to 450 nm (Figure 3). Similar transitions have also been observed in $[Pt(phen)_2]^{2+}$.[16] Since these bands are absent in the free ligand or its protonated form (see Figure 3), we suggest that the transitions involved may contain MLCT character. Such a suggestion is not unreasonable since the MLCT bands of some platinum α-diimines have been claimed to occur around 330 nm for $Pt(bpy)Cl_2$[17] and 440–450 nm for $[Pt(3,3'\text{-}CH_3OCO)bpyCl_2]$.[16d]

Table VI. Luminescence Data in the Solid State and in Solution

property	$[Pt(QP)](ClO_4)_2$ powder	$[Pt(pQP)](ClO_4)_2$ powder	$[Pt(pQP)](ClO_4)_2$ CH_3CN soln
excitation (nm)	355	355	355
λ_{max} (nm)	700	700	496
			533
			573
τ_0 (μs)	0.24 ± 0.01	0.24 ± 0.01	7.0 ± 0.6
ϕ_f			0.026 ± 0.001

Luminescent properties of platinum(II) complexes have been observed in our laboratory[18] and reported by others.[19,20] In this case, both **1** and **2** show weak emission at room temperature. When the spectra were taken at 77 K, a broad emission from 650 to 800 nm was observed (Table VI). Previous studies[16a] showed that the solid sample of $[Pt(phen)_2]^{2+}$ also had a broad peak around 650 nm, which has been attributed to excimeric interaction of the phenanthroline ligands.

One interesting feature of quaterpyridine is its steric rigidity. The strong bonding with platinum not only helps to maintain the planar geometry but also reduces the twisting motion of complexed ligands. This point makes sense as the more sterically hindered **1** emits in solution but not **2**, which has only 5′- and 3″-hydrogens in the conflict region. Figure 4 shows the excitation and emission spectra of **1** measured in degassed acetonitrile at room temperature. The excitation spectrum is vibronically structured (spacing 1200, 1300 cm^{-1}) (Figure 4 and Table VI) and closely matches the 365-nm absorption band shown in Figure 3. The emission centers at around 500 nm are also vibronically structured (spacing 1364 and 1394 cm^{-1}). Self-quenching behavior of the emission has also been observed. The measured self-quenching rate constant determined for solutions from 10^{-4} to 10^{-5} M is (2.9 ± 0.4) × 10^8 M^{-1} s^{-1}; the emission lifetime at infinite dilution (τ_0) is 7.0 μs. The long emission lifetime indicated that the transition involved is a spin-forbidden process. However, we cannot decide whether the emitting state is $^3(\pi\pi^*)$ or ^{3}MLCT.

The cyclic voltammogram of **1** in acetonitrile shows one quasi-reversible reduction couple at –0.19 V, one irreversible reduction

(14) Chassot, L.; Muller, E.; von Zelewsky, A. *Inorg. Chem.* **1984**, *23*, 4249–4253.
(15) Gisselbrecht, J. P.; Gross, M.; Lehn, J. M.; Sauvage, J. P.; Ziessel, R.; Piccinni-Leopardi, C.; Arrieta, J. M.; Germain, G.; Meerssche, M. V. *Nouv. J. Chim.* **1984**, *8*, 661–667.
(16) (a) Miskowski, V. M.; Houlding, V. H. *Inorg. Chem.* **1989**, *28*, 1529–1533. (b) Miskowski, V. M.; Houlding, V. H. *Coord. Chem. Rev.* **1991**, *111*, 145–152. (c) Miskowski, V. M.; Houlding, V. H. *Inorg. Chem.* **1991**, *30*, 4446–4452. (d) Miskowski, V. M.; Houlding, V. H.; Che, C. M.; Wang, Y. To be submitted for publication.
(17) (a) Gidney, P. M.; Gillard, R. D.; Heaton, B. T. *J. Chem. Soc., Dalton Trans.* **1973**, 132–134. (b) Bartocci, C.; Sostero, S.; Traverso, O.; Cox, A.; Kemp, T. J.; Reed, W. J. *J. Chem. Soc., Faraday Trans. 1* **1980**, *76*, 797–803.
(18) (a) Wan, K. T.; Che, C. M.; Cho, K. C. *J. Chem. Soc., Dalton Trans.* **1991**, 1–4. (b) Wan, K. T.; Che, C. M. *J. Chem. Soc., Chem. Commun.* **1990**, 140. (c) Che, C. M.; Wan, K. T.; He, L.-Y.; Poon, C. K.; Yam, V. W. W. *J. Chem. Soc., Chem. Commun.* **1989**, 143.
(19) (a) Zuleta, J. A.; Chesta, C. A.; Eisenberg, R. *J. Am. Chem. Soc.* **1989**, *111*, 8916. (b) Zuleta, J. A.; Burberry, M. S.; Eisenberg, R. *Coord. Chem. Rev.* **1990**, *97*, 47.
(20) (a) Maestri, M.; Sandrini, D.; Balzani, V.; von Zelewsky, A.; Deuschel-Cornioley, C.; Jolliet, P. *Helv. Chim. Acta* **1988**, *71*, 1053. (b) Maestri, M.; Deuschel-Cornioley, C.; von Zelewsky, A. *Coord. Chem. Rev.* **1991**, *111*, 117–123.

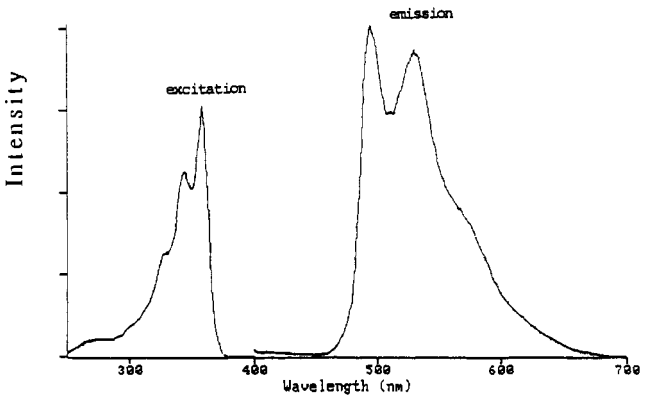

Figure 4. Excitation and emission spectra of $[Pt(pQP)](ClO_4)_2$ in degassed acetonitrile at room temperature.

Scheme I [a]

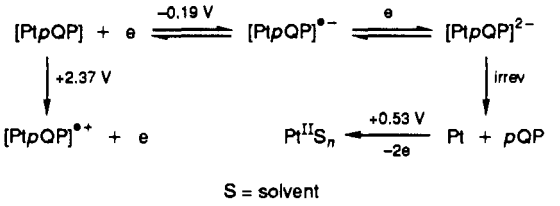

[a] In V vs NHE.

Scheme II

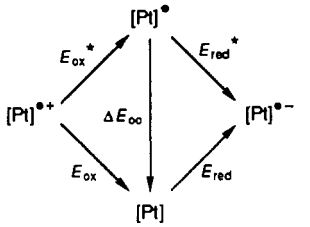

at −1.14 V, and two irreversible oxidations at +0.53 and +2.37 V (against NHE; 0.577 V was used for 0.1 M $AgNO_3$ (CH_3CN)/Ag vs NHE) upon reverse oxidative scan.[3] Scheme I is proposed to account for the above observations.

The oxidation of **1** probably generates Pt(III) (in a formal sense), which is a highly unstable species. This may account for the observed irreversibility in electrochemical oxidation. On the other hand, the electrochemical reduction of **1** at −0.19 V is likely to be ligand centered since a similar reduction couple has also been observed in the related $[Ni(QP)]^{2+}$ complex.[21]

The electrochemical properties of **2** are similar to that of **1**. There are a quasi-reversible couple at E_{pc} = −0.12 V and E_{pa} = +0.07 V, an irreversible reduction wave at −0.98 V, and an irreversible oxidation wave at +0.52 V (vs NHE). It seems likely that the electrochemical properties of **2** could also be described as in Scheme I.

The excited-state potentials corresponding to the processes in Scheme II are calculated with eqs 1 and 2, where ΔE_{00} was

$$E_{ox}^* = E_{ox} - \Delta E_{00} \quad (1)$$

$$E_{red}^* = E_{red} + \Delta E_{00} \quad (2)$$

estimated to be about 2.49 eV from the first emission maximum (496 nm). The estimated E_{ox}^* and E_{red}^* values are about −0.11 and 2.3 V (vs NHE), respectively. Thus, **1** would be a strong photooxidant apart from kinetic requirements.

As the complexes have overall planar structures, we believe they would have interculation phenomena with polynucleic acids. One of our interests is the interaction of DNA with transition metal complexes.[22] In this context, water-soluble triflate salts of **1** and **2** were synthesized and characterized by ^1H NMR (Figure S3) and electronic spectra. The cyclic voltammogram of $[2](CF_3SO_3)_2$ has been measured in pH 6 solution, where a quasi-reversible couple was observed at E_{pc} = −0.15 and E_{pa} = +0.09 V (vs NHE).

It has been shown that bis(2,2′-bipyridine)platinum(II) has fluxional behavior in aqueous medium where hydroxide ion can compete with bipyridine as coordinating ligands.[23] In order to test the flexibility of ligated quaterpyridine, we compared the electronic spectra of triflate salts in different pH solutions by measuring the absorbances at 367 and 333 nm (for **1**) and at 360 and 344 nm (for **2**), respectively. No new absorption peak or absorbance change has been observed within experimental error. These platinum complexes appear to retain the steric integrity from pH 2 to pH 11 at ambient temperature.

The above results indicate that $[1](CF_3SO_3)_2$ may be a good candidate for probing the interaction of planar polypyridine complexes with DNA duplex such as interculation or photochemical activation by observing the change of photoluminescence. Research in this direction will be pursued in the future.

Acknowledgment. We acknowledge support from the Croucher Foundation, The University of Hong Kong, and the National Science Council of Taiwan. C.-M.C. acknowledges the award of a Visiting Professorship administered by the National Science Council of Taiwan.

Supplementary Material Available: Figures S1 and S2 (unit cell packing diagrams) and Figure S3 (^1H NMR spectrum of **1**) and Tables S1–S5, giving crystal data and details of the structure determination, atomic coordinates, hydrogen atom parameters, and anisotropic thermal parameters (9 pages). Ordering information is given on any current masthead page.

(21) Che, C. M. Unpublished result.

(22) Sundquist, W. I.; Lippard, S. J. *Coord. Chem. Rev.* **1990**, *100*, 293–322.
(23) Serpone, N.; Ponterini, G.; Jamieson, M. A.; Bolletta, F.; Maestri, M. *Coord. Chem. Rev.* **1983**, *50*, 209–302.